
Proceedings Paper:
Davila Garcia, M.L., Paredes Soto, D.A. and Mihaylova, L.S. (2018) A Bag of Features Based Approach for Classification of Motile Sperm Cells. In: 2017 IEEE International Conference on Internet of Things (iThings) and IEEE Green Computing and Communications (GreenCom) and IEEE Cyber, Physical and Social Computing (CPSCom) and IEEE Smart Data (SmartData). 10th IEEE International Conference on Cyber, Physical and Social Computing (CPSCom-2017), 21-23 Jun 2017, Exeter, UK. IEEE. ISBN: 978-1-5386-3066-2.

https://doi.org/10.1109/iThings-GreenCom-CPSCom-SmartData.2017.21

A Bag of Features Based Approach for Classification of Motile Sperm Cells

Maria Luisa Davila Garcia, Daniel A. Paredes Soto, Lyudmila S. Mihaylova,
Department of Automatic Control and Systems Engineering, The University of Sheffield, UK
{*mdavilagarcia1, daniel.paredes-soto, l.s.mihaylova*}@sheffield.ac.uk

***Abstract*—The analysis of sperm morphology remains an essential process for diagnosis and treatment of male infertility.**

In this paper, a novel framework based on image processing is proposed to classify sperm cell images affected by noise due to their movement. This represents a challenge, particularly because the cells are not fixed or stained.

The proposed framework is based on Speeded-Up Robust Features (SURF) combined with Bag of Features (BoF) models to quantise features computed by SURF. Support Vector Machines (SVMs) are used to classify the simplified feature vectors, extracted from sperm cell images, into normal, abnormal and non-cell categories. The performance of this framework is compared to a similar model where the Histogram of Oriented Gradients (HOG) is used to extract features and SVMs is applied for their classification.

The proposed framework allows to achieve classification results with an average accuracy of 90% with the SURF approach compared to 78% with the HOG approach.

***Index Terms*—sperm cell; morphology; classification; SURF; HOG; bag of visual features; feature extraction**

I. Introduction

Medical systems require processing of a large amount of data. However, this poses a significant challenge to medical professionals and makes even impossible for a human to analyse this information precisely and reliably. This paper presents an approach for the automated analysis and classification of motile sperm cells.

Sperm cell concentration, morphology and motility estimates are, among other parameters, essential for diagnosis and treatment of male infertility according to the World Health Organization (WHO) [1]. Nowadays, analysis of sperm cells remains subjective, imprecise, and highly time-consuming task [2]. A health professional, usually using a microscope, counts and evaluates the morphology of cells following guidelines established by the WHO [1] and based on their own experience.

Computer-Assisted Semen Analysis (CASA) systems have been used at andrology laboratories and Assisted Reproductive Units (ARU) world-wide in the last decades. Nevertheless, CASA systems represent a high-cost and frequently lack for adaptive methods able to work under a variety of conditions, since sperm sample vary significantly.

Over the last years, a wide range of works aim to achieve accurate and robust morphology classification of sperm cell. These include not only human sperm cell, but also different species [3], [4] and other biological particles: virus, bacteria, stem cells [5] and tumour images [6].

Methods for assisted conception such as Intra-Cytoplasmatic Sperm Injection (ICSI) and *in-vitro* fertilisation (IVF) require a selection of a few sperm cells for the fertilisation. In ICSI, for instance, an embryologist selects the best normal-looking sperm cells under high magnification. It has been found that morphology can be associated to the sperm cell function including the ability for fertilisation (based on statistical estimates only) [7], [8], [9]. Hence, morphology measurements play an important role to select the best sperm cells [10].

Motile sperm cells can be labelled as normal or abnormal based on its morphology, by fulfilling the strict WHO references [1], and their motility grade. A formal definition for normal morphology of sperm cells is presented by Menkveld *et al.* [11] and it is described as follows. The head is if length between 3 and 5 μm and the width is between 2 and 3 μm. The head has to contain a well-defined acrosomal region and the sperm tail measuring 45 μm in length with a uniform width.

Also, motility of sperm cells can be affected by physical characteristics of the seminal fluid (*e.g.* viscosity and pH), sperm cell variables (*e.g.* sperm concentration) and the presence of debris [1]. Those conditions can produce noise and changes in illumination when images are captured making automated sperm cell detection difficult. In addition, we need to consider the noise introduced by imaging devices during the image formation process in the hardware used.

Staining procedures using compounds have been reported improving sperm cell segmentation due to the large colour contrast produced between live sperm cells and the background in images. Nevertheless, staining of sperm cells have also been reported to cause morphology alterations, specifically changes in their head [12].

Appearance of sperm cells in video sequences can change due to the conditions at every scene captured. Variation of illumination resulting from the flow of the seminal fluid, for instance, can produce shades in the background. Focus drift from the temperature gradient and mechanical vibrations in the microscope can affect the sharpness of the elements in the image [13], [14]. Also, the movement of sperm cells can occur at any orientation in samples where no attracting source is utilised. Thus, the shape and size of sperm cells can be visually different when they move orthogonally to the camera plane.

The framework presented is this paper integrates SURF, Bag of Features and Support Vector Machine for the classification

of sperm cell in microscopy images based on low-level features. The approach proposed is able to analyse images from unstained and motile sperm cells.

The rest of this paper is organised as follows: Section II describes foundations of Histogram of Oriented Gradientes (HOG), Speed-Up Robust Features (SURF) and Bag-of-Features (BoF) methods and some works related. In Section III, the proposed approach is developed. Experimental results are presented in Section IV and Section V summarises the work.

II. Related Works

Digital image processing methods can be used to detect and classify objects based on low-level features in microscopy images. The approach proposed in this paper combines a set of algorithms to extract and organise features of sperm cell images to train a classifier. A SVM algorithm is used to classify features from new image samples into one of the following classes: *normal-, abnormal-* and *non-sperm cell*.

A. Histogram of Oriented Gradients

A Histogram of Oriented Gradients (HOG) was introduced by Dalal *et al.* [15] for human silhouette detection. Nowadays its use has been extended to other areas such as text and face recognition [16], [17]. The HOG is based on the distribution of intensities of gradients G_x and G_y of a given image. Gradient estimates at a pixel(i, j) are given by (1) and (2).

$$G_{x(i,j)} = f\left(i+1, j\right) - f\left(i-1, j\right), \tag{1}$$

$$G_{y(i,j)} = f\left(i, j+1\right) - f\left(i, j-1\right) \tag{2}$$

where $f\left(i, j\right)$ is the intensity value at pixel location (i, j). Gradients can be used to estimate the local orientation θ and magnitude H of the gradient:

$$\theta\left(i, j\right) = arctan(G_{x(i,j)}/G_{y(i,j)}), \tag{3}$$

$$H\left(i, j\right) = \sqrt{G^2_{x(i,j)} + G^2_{y(i,j)}} \tag{4}$$

To compute the HOG of a given image, it is divided into small regions termed cells. Orientation of gradients are computed and the histogram of the gradients is calculated. Gradient can be performed by filtering the image using a Sobel-based kernel $D_x = [-1 \quad 0 \quad 1]$ and $D_y = [-1 \quad 0 \quad 1]^T$. The concatenation of all histograms produces the feature vector of the image.

A visualisation of HOG features extracted from a normal sperm cell using a patch size of 4×4 and 8×8 pixel units is shown in Figure 1.

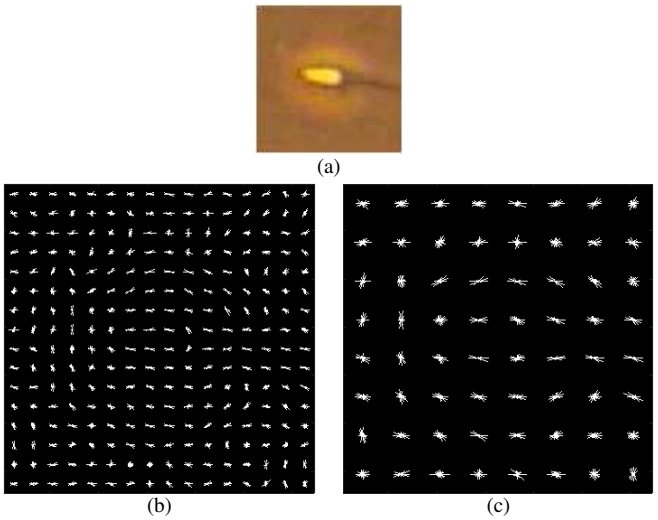

Fig. 1. Visualization of HOG features: (a) Original image, (b) HOG using a patch size of 4×4 and (c) using a patch size of 8×8.

B. Speeded-Up Robust Features

Speeded-Up Robust Features (SURF)—based on the Scale-Invariant Feature Transform (SIFT) [18]—was introduced by Bay *et al.* [19] and has been shown to be successful in object recognition approaches [20].

Mehrotra *et al.* [21], for instance, use an adaptive SURF descriptor for human iris recognition; Feulner *et al.* [22] employ SURF for human-body region detection in Computed Tomography (CT) data; and, Han *et al.* [23] use SURF for traffic sign recognition in colour images.

Similarly to SIFT [24], SURF analyses the spatial distribution of gradients. In addition, SURF divides the image in sub-regions that make the method faster and less noise-sensitive [19]. SURF is based on the Hessian matrix and relies on its determinant to select the best response across a range of scales. Hence, it integrates the scale-space theory introduced by Lindeberg [25]. The Hessian matrix $\mathcal{H}\left(\mathrm{x}, \sigma\right)$ at a location with pixel coordinates $\mathrm{x} = (x, y)$ and scale σ in an image I is given by (5).

$$\mathcal{H}\left(\mathrm{x}, \sigma\right) = \begin{bmatrix} L_{xx}\left(\mathrm{x}, \sigma\right) & L_{xy}\left(\mathrm{x}, \sigma\right) \\ L_{xy}\left(\mathrm{x}, \sigma\right) & L_{yy}\left(\mathrm{x}, \sigma\right) \end{bmatrix} \tag{5}$$

where $L_{xx}\left(\mathrm{x}, \sigma\right)$ is the second-order partial derivative $\frac{\partial^2}{\partial x^2} g(\alpha)$ with the image I at point x and can be estimated by the convolution of I with a second-order derivative of a Gaussian kernel, also known as Laplacian of Gaussian (LoG); $L_{yy}\left(\mathrm{x}, \sigma\right)$ and $L_{xy}\left(\mathrm{x}, \sigma\right)$ can be estimated similarly. Unlike SIFT, SURF estimates the second-order Gaussian derivatives using box filters based on integral images.

C. Bag of Features

Bag of Features (BoF)—originally called Bag of Words (BoW) [26]—was first introduced to natural language processing, text-mining and linguistic methods. Later, BoF is adapted and proposed by Csurka *et al.* [27] for visual categorisation. BoF has been widely used. Shen *et al.* [28], for instance, use BoW for classification of cells in biomedical images. Zhou [29] and Nanni *et al.* [30] employ BoF to classify scenes contained in images.

BoF aims to represent the extracted features of an image as a histogram of the computed features by quantising the features. The BoF model for sperm cell images classification is summarised in the following steps:

1) *Selection of features.* In this paper, the SURF method is used to extract the strongest key points representing an image. A small region (patch) surrounding every key point is selected to extract the image features.
2) *Learning vocabulary—also termed visual codebook.* In this step, the extracted features are divided into groups (clusters). The clustering process can be carried out by using the K-means approach, where the centroid of a cluster represents a visual word of the codebook [31].
3) *Feature quantisation.* The final step in the BoF model is the mapping process of every feature (patch) into a specific codeword by using a distance metric (*e.g.* Manhattan or Euclidean). Finally, quantisation of features yields the histogram representation of the codewords.

III. The Proposed Framework for Sperm Cells Classification

The proposed method for sperm cell classification is summarised in Figure 2 and each step is described in the following sections.

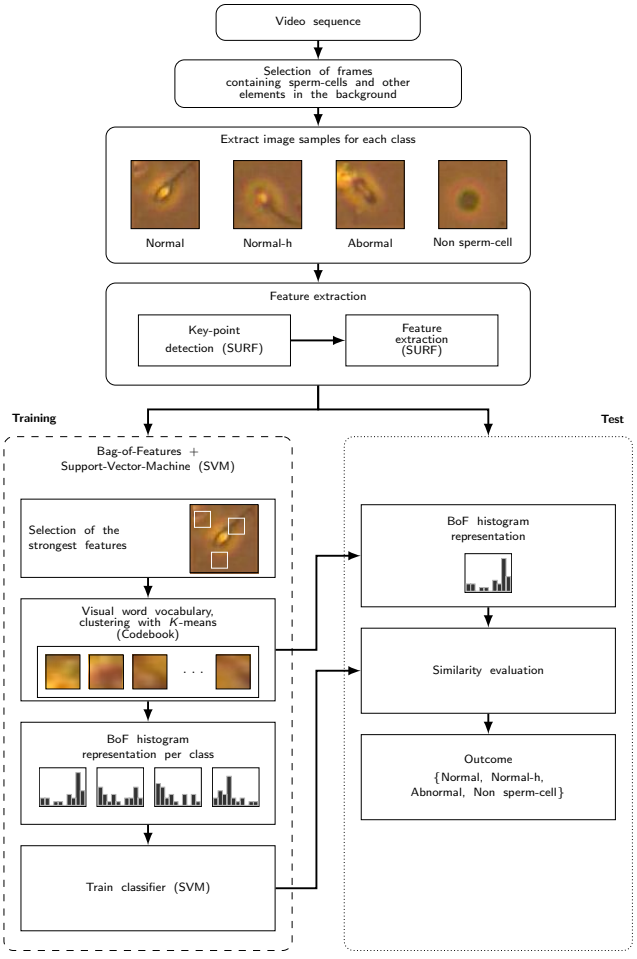

Fig. 2. Proposed framework for unstained sperm cell classification based on SURF, Bag-of-Features and SVM classifier.

A. Template definition

Appearance of sperm cells (*e.g.* area and eccentricity) can change over time due to their movement, the static position of the observer and the representation of a 3D space onto a plane (image). In Figure 3, for instance, a set of two *normal* sperm cells along a sequence of five consecutive frames is shown. The variation in size and brightness can be observed as sperm cells swim. Note that sperm cells were not stained or altered in the current work. Those visual artefacts can challenge the methods used to automate the classification of sperm cells.

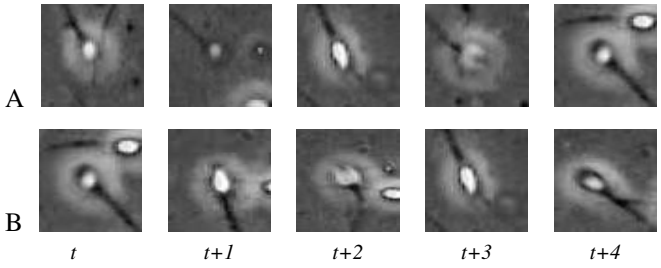

Fig. 3. Appearance variation of two sperm cells (upper and lower row) along consecutive video frames $t \in [0, 1, ..., 4]$.

In Figure 3, a 'halo' surrounding sperm's head can be observed in some images making head's edge difficult to distinguish. Therefore, the variation in the sharpness of sperm-cell's head is considered into the definition of a normal sperm cell in this paper.

The sperm cell images are categorised into the following classes:

- Normal. Sperm cell matching the normal morphology criteria and with a sharp head's edge.
- Normal-h. Normal sperm cell with a blurred head's edge.
- Abnormal. Sperm cell that does not meet the normal morphology definition.
- Other. Other component in debris or uniform patch.

Figure 4 shows sperm cell examples of the classes described above.

B. Datasets

A collection of video frames showing sperm cells and other objects are selected to create two datasets: training and testing. Image patches containing a single sperm cell are selected for the different classes defined. The patches are manually selected to include the possible variates that can be found in practice (*e.g.* orientation and morphology of sperm cells and other objects in the background). The testing dataset is used to validate and measure the performance of the method proposed.

C. Feature extraction

The SURF [19] method is used to detect key points from the images. SURF selects the most representative pixels based in low-level features—using the Hessian matrix. Even though SURF is invariant to rotation, sperm cell samples at different orientations are used to consider the pixellation effect when capturing the images. For every key point, the SURF features

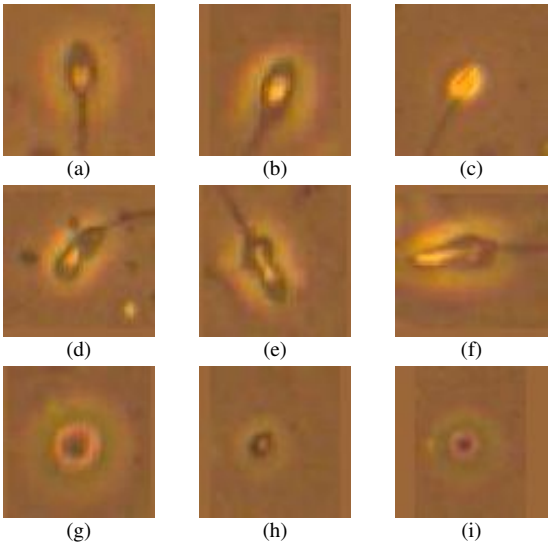

Fig. 4. Sperm cell samples from the four categories defined: (a),(b) normal; (c) normal-h; (d)-(f) abnormal; (g)-(i) other components in debris.

are computed using a region of $m \times n$ pixels encompassing the key point location yielding to the initial feature vector.

D. Training

1) Selection of the strongest features: The number of features is reduced by selecting the minimal number of features n found across the four classes. The SURF method is used to choose the n strongest features from each image. Thus, the same number of features for each image across all classes can be transferred to the training process of a classifier.

2) Bag-of-Features (BoF): Processing large SURF vectors can represent a high computational cost. Hence, the BoF model is employed to reduce the feature representation of the images. The aim of BoF is creating a codebook—also termed Visual Word Vocabulary—by transforming feature vectors into visual words. In order to do so, the SURF feature vectors are clustered by using *K*-means. The number of clusters *K* defines the codebook size and the centroids of clusters define the words.

Thus, each feature of the SURF vectors is assigned to one word. This can be represented by a histogram where the $x-$axis represents the words and $y-$axis the number of features mapped to the words (see Figure 5). The BoF method is repeated to produce the histogram of BoF for each of the four classes defined. The resulting BoF model is used to train the classifier.

3) Training of a Support Vector Machine (SVM) classifier: A multi-class Support Vector Machine (SVM) classifier is trained with the BoF model obtained. SVMs are inherently binary classifiers. Thus, an approach is set-up to define the class for a new entry. A 'one-to-one' model is used to define the outcome based on the most voted class by the binary classifiers. The trained SVM model is used to process BoF histograms instances from the training dataset.

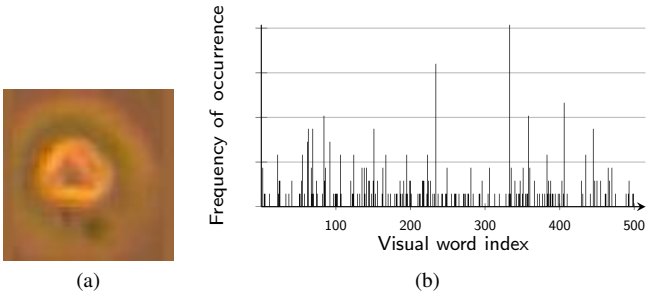

(a) (b)

Fig. 5. Normalised BoF histogram using SURF features from a non-cell sample image. (a) Original image, (b) BoF histogram using 500 words.

E. Test

For each image in the testing dataset, the BoF histogram is computed as follows: Using the BoF model—codebook, a histogram is computed by mapping every SURF feature to a word in the codebook. The distance $l_2 - norm$ is used to estimate the closest distance between a feature and the words in the codebook. The resulting histogram is normalised and classified by the SVM model which eventually measures the similarity to the class models obtained in the training process.

IV. Experiments and Results

A. Experimental Set-up

Sperm samples used for this research are obtained from donors at the Academic Unit of Reproductive and Developmental Medicine (AURDM) of the University of Sheffield in the UK. All of donors provided explicit consent to use their samples for research purposes only. The sperm samples were not prepared or pre-processes (diluted, stained or altered to re-orientate their direction.)

Microscopy video sequences are recorded at a rate of 10 frames per second producing 8-bit colour images of 2040 x 1086 pixels in size. Sperm cell samples for both, training and testing, are extracted from frames which were selected by using a random function. A full dataset—images of all classes—is formed by: 235 images labelled as *normal*; 235 *normal-h*; 235 *abnormal*; and, 235 images containing other objects considered as *non-cell*.

The labelling process is based on the WHO guidelines and the visual appearance of the sperm cell images. The images ranged from 60×60 to 70×85 pixels in size and are compressed into JPEG (Joint Photographic Experts Group) format.

In this paper, 235 images are used for each class. This process aims to make a fear comparison between the number of features for each class in the training process.

The full dataset is divided into two datasets: 30% of the images were used for training and 70% for testing.

B. Performance evaluation

The parameters of the implemented methods are chosen accordingly. The 95% of the strongest SURF features are used to choose a reduced number of features which are used by the

BoF method. A *K*=2325 is used in the *K*-means clustering process to create a BoF model which is passed to an SVM classifier—based on a $K(K1)/2$ kernel—for training.

The performance obtained with the framework proposed reached an average accuracy of 90%. The average accuracy is defined as the mean between the accuracy of each class, in this case, it is given by the sum of the values along the major diagonal divided by the number of classes, 4. The confusion matrix of the proposed classification method is presented in Table I. Elements along the major diagonal represent the accuracy of the classifier.

TABLE I
CONFUSION MATRIX FOR TESTED CELLS USING SURF

	Abnormal	Non-Cell	Normal	Normal-h
Abnormal	**0.87**	0.11	0.02	0
Non-Cell	0.02	**0.97**	0	0.02
Normal	0.06	0	**0.87**	0.06
Normal-h	0	0.05	0.06	**0.89**

The confusion matrix relies on the four possible outcomes given a classifier and an instance—image patch. If the image patch, e.g. normal sperm cell, is classified correctly, it is counted as a true positive (TP). If it is wrongly classified, e.g. if the normal sperm cell is labelled as normal-h, abnormal or non sperm cell, it is counted as a false negative (FN). If the image patch is a negative instance, e.g. containing any of the other three classes: normal-h, abnormal or non sperm cell, and it is classified as negative—non normal sperm cell, it is counted as true negative (TN). If the same negative instance is classified as positive—normal sperm cell, it is counted as false positive (FP).

The confusion matrix can be used to calculate common metrics to measure the performance of the classifier as described below.

The accuracy (Ac) is characterized by (6) and measures the degree of correct classification [32].

$$Ac = \frac{TP+TN}{P+N} = \frac{TP+TN}{TP+TN+FP+FN}. \quad (6)$$

where the positives (P) are determined by FN and TP, and the negatives (N) are determined by TN and FP.

The precision of a measurement is the degree of repeatability of a measurement and it is calculated by (7).

$$Pre = \frac{TP}{TP+FP} \quad (7)$$

Recall or sensitivity is also known as the true positive rate (TPR). It measures the proportion of TP which are correctly identified as positives [32]. The recall (Rec) is given by (8).

$$Rec = \frac{TP}{P} = \frac{TP}{TP+FN}. \quad (8)$$

The F-measure metric is derived from the precision and recall estimates as a ratio between two effectiveness measures [33]. It is calculated by (9).

$$F - measure = 2 \times \frac{Pre \times Rec}{Pre + Rec} \quad (9)$$

The results from this performance measures are summarised in Figure 6.

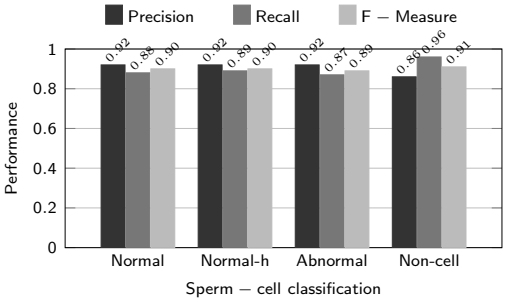

Fig. 6. Performance of the proposed classification method based on SURF, BoF and SVMs.

The performance of the framework proposed is compared to an approach based on HOG combined with SVM, where HOG is used to extract feature vectors directly from images. The confusion matrix of a classification based on HOG features alone is shown in Table II.

TABLE II
CONFUSION MATRIX FOR TESTED CELLS USING HOG

	Abnormal	Non-Cell	Normal	Normal-h
Abnormal	**0.75**	0.01	0.01	0.05
Non-Cell	0.05	**0.81**	0	0.14
Normal	0.10	0.10	**0.75**	0.05
Normal-h	0.05	0	0.15	**0.80**

The average accuracy overall classes reached the 78%. Performance metrics estimates are summarised in Figure 7.

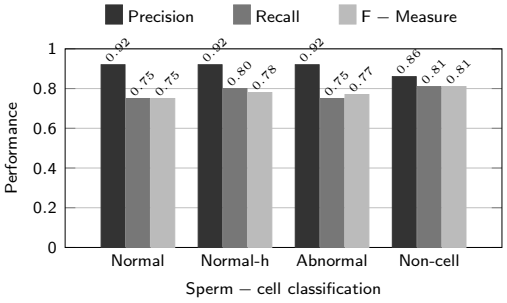

Fig. 7. Performance of a comparative classification method based on HOG and SVMs.

V. SUMMARY

In this paper, we propose a fast and efficient framework for sperm cells classification. Our approach combines the Bag of Features model where SURF features have been clustered using *K*-means into a visual words.

This paper proposes a reliable approach to analyse the large amount of data generated from the SURF feature extraction. The analysis comprises the selection of the most representative features that best describe each of the four classes defined in this work for the classification of new instances.

The best performance is obtained when we define a vocabulary size equal to 2325 keeping 95% of strongest features for the codebook.

The proposed framework allows achieving an average classification accuracy of 90% outperforming a similar approach based on HOG for feature extraction which has shown 78% average classification accuracy.

ACKNOWLEDGMENT

The authors gratefully acknowledge the financial support of the Mexican Consejo Nacional de Ciencia y Tecnología (CONACYT). We also acknowledge the Andrology laboratory of the Academic Unit of Reproductive and Developmental Medicine (University of Sheffield) and especially to Prof. Allan Pacey.

REFERENCES

[1] W. H. Organization, *WHO Laboratory Manual for the Examination and Processing of Human Semen*. World Health Organization, 2010.

[2] H. F. Yang, X. Descombes, S. Prigent, G. Malandain, X. Druart, and F. Plourabou, "Head tracking and flagellum tracing for sperm motility analysis," in *Proc IEEE 11th International Symposium on Biomedical Imaging*, 2014, pp. 310–313.

[3] O. Simonik, J. Sichtar, A. Krejcarkova, and Rajmon, "Computer assisted sperm analysis the relationship to bull field fertility , possible errors and their impact on outputs : A review," *Indian Journal of Animal Sciences*, vol. 85, no. January, pp. 3–11, 2015.

[4] P. Kathiravan, J. Kalatharan, G. Karthikeya, K. Rengarajan, and G. Kadirvel, "Objective sperm motion analysis to assess dairy bull fertility using computer-aided system - a review," *Reproduction in Domestic Animals*, vol. 46, no. 1, pp. 165–172, feb 2011.

[5] P. Bajcsy, A. Cardone, J. Chalfoun, D. Juba, M. Majurski, A. Peskin, and Simon, "Survey statistics of automated segmentations applied to optical imaging of mammalian cells," *BMC Bioinformatics*, 2015.

[6] F. X. Su Hai and L. Yang, "Robust cell detection of histopathological brain tumor images using sparse reconstruction and adaptive dictionary selection," *Medical Imaging, IEEE Transactions*, vol. 35, no. 6, pp. 1575–1586, 2016.

[7] K. Lundin, B. Sderlund, and L. Hamberger, "The relationship between sperm morphology and rates of fertilization, pregnancy and spontaneous abortion in an in-vitro fertilization/intracytoplasmic sperm injection programme," *Human Reproduction*, vol. 12, no. 12, pp. 2676–2681, 1997.

[8] D. R. Grow, S. Oehninger, H. J. Seltman, J. P. Toner, R. J. Swanson, T. F. Kruger, and S. J. Muasher, "Sperm morphology as diagnosed by strict criteria: probing the impact of teratozoospermia on fertilization rate and pregnancy outcome in a large in vitro fertilization population," *Fertility and Sterility*, vol. 62, no. 3, pp. 559–567, 1994.

[9] S. Oehninger, A. A. Acosta, M. Morshedi, L. Veeck, R. J. Swanson, K. Simmons, and Z. Rosenwaks, "Corrective measures and pregnancy outcome in in vitro fertilization in patients with severe sperm morphology abnormalities," *Fertility and Sterility*, vol. 50, no. 2, pp. 283–287, 1988.

[10] A. S. Hamberger L., K. Lundin and B. Soderlund, "Indications for intracytoplasmic sperm injection," *Human Reproduction*, vol. 13, no. 6, pp. 128–133, 1998.

[11] T. K. Menkveld R, F. Stander and T. Kruger, "The evaluation of morphological characteristics of human spermatozoa according to stricter criteria," *Human Reproduction*, vol. 5, no. 5, pp. 586–592, 1990.

[12] L. Maree, S. S. du Plessis, R. Menkveld, and G. van der Horst, "Morphometric dimensions of the human sperm head depend on the staining method used," *Human Reproduction*, vol. 25, no. 6, pp. 1369–1382, 2010.

[13] M. Gabriel, D. Balle, S. Bigault, C. Pornin, S. Gétin, F. Perraut, M. R. Block, F. Chatelain, N. Picollet-D'hahan, X. Gidrol, and V. Haguet, "Time-lapse contact microscopy of cell cultures based on non-coherent illumination," *Scientific Reports*, vol. 5, no. 1, 2015.

[14] WHO, *WHO Laboratory Manual for the Examination and Processing of Human Semen*, ser. Nonserial Publications Series. World Health Organization, 2010.

[15] N. Dalal, B. Triggs, and C. Schmid, "Human detection using oriented histograms of flow and appearance," in *Proc of the European Conference on Computer Vision*. Springer Berlin Heidelberg, 2006, pp. 428–441.

[16] S. Tian, S. Lu, B. Su, and C. L. Tan, "Scene text recognition using co-occurrence of histogram of oriented gradients," in *Proc of the 12th International Conference on Document Analysis and Recognition*, Aug 2013, pp. 912–916.

[17] O. Déniz, G. Bueno, J. Salido, and F. D. la Torre, "Face recognition using histograms of oriented gradients," *Pattern Recognition Letters*, vol. 32, no. 12, pp. 1598–1603, sep 2011.

[18] D. G. Lowe, "Object recognition from local scale-invariant features," in *Proc of the IEEE International Conference on Computer Vision*, vol. 2, 1999, pp. 1150–1157.

[19] H. Bay, A. Ess, T. Tuytelaars, and L. V. Gool, "Speeded-up robust features (SURF)," *Computer Vision and Image Understanding*, vol. 110, no. 3, pp. 346–359, jun 2008.

[20] F. Lecron, M. Benjelloun, and S. Mahmoudi, *Descriptive Image Feature for Object Detection in Medical Images*. Berlin, Heidelberg: Springer Berlin Heidelberg, 2012, pp. 331–338.

[21] H. Mehrotra, P. K. Sa, and B. Majhi, "Fast segmentation and adaptive surf descriptor for iris recognition," *Mathematical and Computer Modelling*, vol. 58, no. 12, pp. 132–146, 2013.

[22] J. Feulner, S. Zhou, E. Angelopoulou, and S. Seifert, "Comparing axial CT slices in quantized n-dimensional SURF descriptor space to estimate the visible body region," *Computerized Medical Imaging and Graphics*, vol. 35, no. 3, pp. 227–236, Apr 2011.

[23] Y. Han, K. Virupakshappa, and E. Oruklu, "Robust traffic sign recognition with feature extraction and k-nn classification methods," in *Proc of the IEEE International Conference on Electro/Information Technology*, May 2015, pp. 484–488.

[24] D. G. Lowe, "Distinctive image features from scale-invariant keypoints," *International Journal of Computer Vision*, vol. 60, no. 2, pp. 91–110, 2004.

[25] T. Lindeberg, "Feature detection with automatic scale selection," *International Journal of Computer Vision*, vol. 30, no. 2, pp. 79–116, 1998.

[26] Y. Liu, H. Zha, and H. Qin, "Shape topics: A compact representation and new algorithms for 3d partial shape retrieval," in *Proc of the 2006 IEEE Computer Society Conference on Computer Vision and Pattern Recognition*, vol. 2, 2006, pp. 2025–2032.

[27] G. Csurka, C. R. Dance, L. Fan, J. Willamowski, and C. Bray, "Visual categorization with bags of keypoints," in *Proc of the Workshop on Statistical Learning in Computer Vision*, no. 1-22, 2004, pp. 1–2.

[28] L. Shen, J. Lin, S. Wu, and S. Yu, "Hep-2 image classification using intensity order pooling based features and bag of words," *Pattern Recognition*, vol. 47, no. 7, pp. 2419–2427, 2014.

[29] L. Zhou, Z. Zhou, and D. Hu, "Scene classification using a multi-resolution bag-of-features model," *Pattern Recognition*, vol. 46, no. 1, pp. 424–433, 2013.

[30] L. Nanni and A. Lumini, "Heterogeneous bag-of-features for object/scene recognition," *Applied Soft Computing*, vol. 13, no. 4, pp. 2171–2178, 2013.

[31] S. O'Hara and B. A. Draper, "Introduction to the bag of features paradigm for image classification and retrieval," *CoRR*, vol. abs/1101.3354, 2011.

[32] J. R. Taylor and W. Thompson, "An introduction to error analysis: The study of uncertainties in physical measurements," *Physics Today*, vol. 51, no. 1, pp. 57–58, jan 1998.

[33] D. M. W. Powers, "Evaluation: from precision, recall and f-measure to roc, informedness, markedness and correlation," *International Journal of Machine Learning Technology*, vol. 2, no. 1, pp. 37–63, 2011.